

PHOTO LICENSED BY GRAPHIC STOCK

**T**ODAY'S INDUSTRY AND PERSONAL medical care both strongly demand accurate, reliable, robust, low-power, and low-cost methods to sense changes in the environment and the condition of the body. This is where the concept of smart skin comes in. Smart skins can monitor changes in environmental parameters, such as temperature, strain, and the presence of ambient gas, and communicate these parameters' changes wirelessly or wired, as demonstrated in Figure 1. The smart skin concept can also be extended to that of wearable electronic devices for continuous monitoring and reporting of critical biosignals. There are a lot of challenges for the state of the art of smart skin, such as expensive fabrication methods, a lack of flexibility and mobility, and the large area fabrication method. This

article presents novel wireless smart skins that employ an ink-jet printing additive manufacturing technique in large areas for sensing ambient gases. These skins can be applied in both industry and commercial uses. The skins scavenge energy

using ambient electromagnetic, solar, thermal, mechanical, or radio-frequency identification (RFID)/radar-based interrogation techniques. In short, these smart skins could prove to be the ultimate sensing tool that could potentially allow for

## Smart Skins

Could they be the ultimate sensing tool?

TAORAN LE, ZIYIN LIN, C.P. WONG, AND M.M. TENTZERIS

the mass implementation of a perpetual wireless network even in extremely rugged environments.

Carbon nanomaterials, such as single-walled carbon nanotubes (SWCNTs), multiwalled CNTs, and graphene, have been considered and investigated as candidates for the quick and precise detection of various chemicals [1]–[3]. Because of their large surface area, carbon nanomaterials have the ability to physically and chemically absorb the chemicals on their surface [4], [5]; these carbon nanomaterials then alter their properties, which is the foundation for the chemical sensor applications [6], [7]. The absorption of the chemical compounds causes changes in the material and electrical properties such as dc resistance, real and imaginary parts of the impedance, and an effective dielectric constant [1]. These electrical changes can determine the presence of various chemicals by measuring electrical quantities such as changes in the current, resonant frequency, and amplitude of backscattered power. Their light weight, low cost, outstanding electrical conductivity, and ease of fictionalization targeted for a broad range of chemicals make these carbon materials ideal candidates for the development of a wide spectrum of portable and wearable sensors. All of these sensors can build up smart skins. Moreover, the compatibility of these materials to be applied via direct-write methodologies on low-cost, flexible, and environmentally friendly substrates provides the ability to mass produce commercial devices at a low cost.

### INK-JET PRINTING: A NOVEL ADDITIVE MANUFACTURING FABRICATION TECHNIQUE

Before going into the intricacies of the sensors and wireless sensing mechanisms that enable smart skins, a step back will be taken that makes smart skins feasible in a cost-effective way for applications up to tens of gigahertz, which is ink-jet printing. The traditional wet-etching techniques that form the backbone of the conventional printed circuit board (PCB) fabrication process involve the complete metallization of substrate laminates and subsequent selective etching of portions of the metal layer on top of

Their light weight, low cost, outstanding electrical conductivity, and ease of fictionalization targeted for a broad range of chemicals make these carbon materials ideal candidates for the development of a wide spectrum of portable and wearable sensors.

the substrate using etchants. In addition, milling machines are also used to realize circuits on metal-laminated substrates.

They operate like plotting machines with milling bits that selectively remove unwanted metal from the PCB boards.

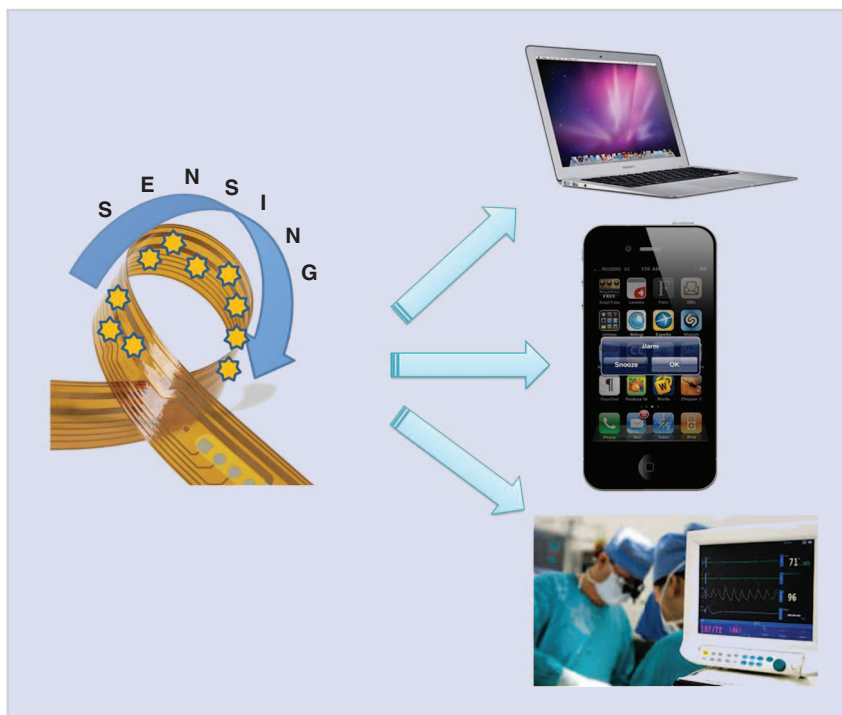


FIGURE 1 The smart skin module.

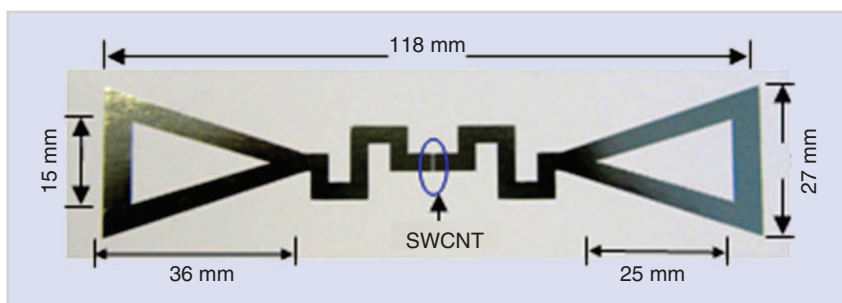
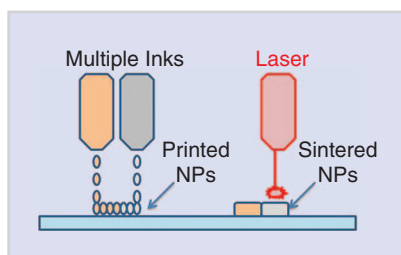


FIGURE 2 An ink-jet-printed, RFID-enabled, CNT-based wireless sensor tag.



**FIGURE 3** A diagram of an inline laser sintering process to anneal printed nanoparticles (NPs).

Both methods create a significant amount of waste during the fabrication process.

Ink-jet-printing conductive materials over a substrate offers substantial benefits over the conventional subtractive methods in terms of reduced waste and ease of fabrication. It typically uses an electrostatic potential (normally 5–12 V) difference between a charged electrode attached to the ink cartridge and the base plate on which the substrate is mounted [8]. The cost-effective and green nature of ink-jet printing technology as a fabrication method on low-cost, organic flexible substrates such as paper make it ideal for large-scale reel-to-reel processing with high repeatability.

One of the biggest issues that inhibited the advancement of smart skins in the past was the inability to fabricate on conformal large-area substrates. The typical fabrication process on flexible substrates takes place in a clean-room environment or is a subtractive process, such as patterning and etching [9]. This is not only an expensive process, but it has detrimental environmental effects due to the hazardous chemicals required. It is a very wasteful approach, especially for circuits that do not contain large metal areas. The ink-jet printing technique is a

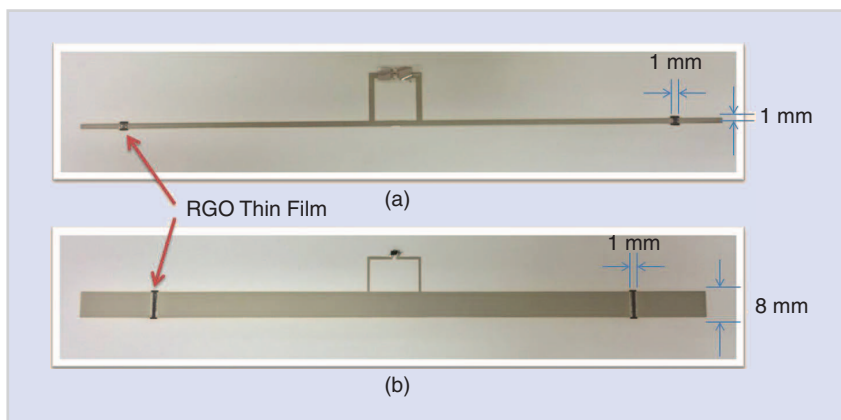


**FIGURE 4** The antenna tags with the RFID integrated circuit printed on photo paper with different RGO sensing areas.

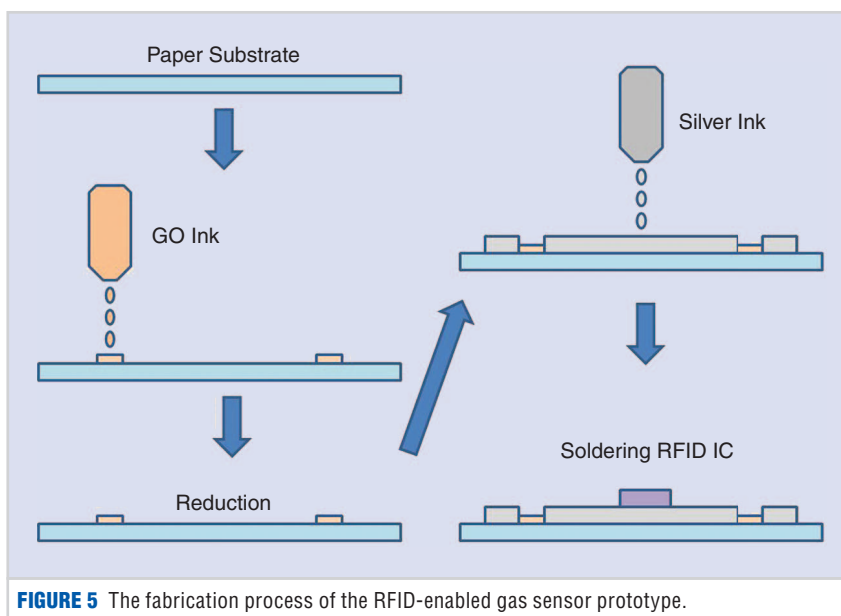


**FIGURE 5** The fabrication process of the RFID-enabled gas sensor prototype.

good method for the fabrication of large-area circuits that do not contain large metal areas, such as wireless sensors and three-dimensional radio-frequency (RF) communication and control modules. Over the last

decade, major advances in printing technology have pushed printing into the mainstream for the fabrication of flexible and conformal electronics because it eliminates the majority of these issues. Roll-to-roll technology can print conformal skins that are hundreds of meters long and, in some cases, kilometers if required. It can also be used with low-cost organic and polymer substrates such as paper, which have the potential to create “green” smart skins if effective environmentally friendly protective coatings are applied.

Previously, we investigated the electrical characteristics of paper for the first time in the ultrahigh-frequency (UHF) range and have used it to design and fabricate RFID tags and RF sensors by ink-jet printing. One of them is shown in Figure 2, which

**Carbon nanomaterials, such as single-walled carbon nanotubes (SWCNTs), multiwalled CNTs, and graphene, have been considered and investigated as candidates for the quick and precise detection of various chemicals.**

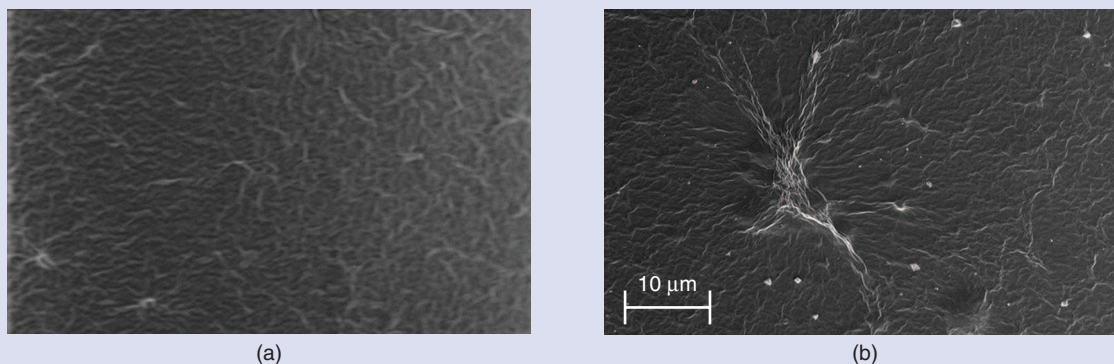


**FIGURE 6** (a) The printed GO before reduction and (b) the reduced GO [2].

presents an ink-jet-printed RFID sensor tag with a printed SWCNT film on a flexible paper substrate [10]. The operation principle of the proposed CNT-based sensor uses the same backscattering principles that are currently in use with existing RFIDs to communicate the data from the passive tag to a reader [10].

Ink-jet printing of electronics has been enabled by the discovery of printable conductive nanoparticles. In [11], we characterized the silver ink conductivity up to 12.5 GHz, and the highest conductivity by ink-jet printing achieved  $1.1 \times 10^7$  S/m. These nanoinks also consist of nanometer-sized particles of CNTs, graphene, or a wide range of semiconducting and polymer compounds in addition to metals. The particles must be small enough to be printed through the micron-sized nozzles of an ink-jet printer head. Several nozzles can be run at once to pattern multiple materials simultaneously. Once the materials are patterned onto the substrate, a curing process, such as heat, laser, or atmospheric modification, melts or links the printed nanoparticles into bulk structures [11]–[13]. The entire process can be completed in a matter of minutes, allowing for rapid production at a large scale. An example of this process is shown in Figure 3. Because of the wide variety of materials this process can deposit, the use of nanoenabled ink has become popular for printing RFID-based antennas, sensors, and even CNT-based diodes and transistors [14]–[16]. This makes printing a proper process to integrate monolithic integrated sensors, antennas, and RFIDs into smart skins.

To demonstrate the printability of carbon-based nanoparticle ink, we present a preliminary prototype in Figure 4, which is made from reduced graphene oxide (RGO) directly deposited onto Kodak photo paper. Graphene was chosen because of its special electronic and mechanical properties [3], [7]. Graphene is a single planar layer of carbon atoms with exotic physical properties including a high mobility of charge carriers ( $200,000 \text{ cm}^2 \text{ V}^{-1} \text{ s}^{-1}$ ) and high thermal conductivity ( $\sim 5,000 \text{ W m}^{-1} \text{ K}^{-1}$ ). Most importantly, as a zero-bandgap semiconductor, graphene's high metallic conductivity and low-charge carrier density enable extremely high sensitivity because small variations in the charge carrier density yield

notable changes in conductivity [3]. Unlike pristine graphene, which has very poor dispersion in water, graphene oxide (GO) exhibits excellent solubility in water because of the existence of hydrophilic functional groups on the surface [17], rendering it an excellent candidate for the development of environmentally friendly water-based inks. Cabot's CCI-300 conductive silver nanoparticle ink was used to print the external circuitry—a dipole antenna here and the interconnect between the RGO thin film and the antenna.

This fabrication process, shown in Figure 5, includes:

- 1) deposition of the GO ink on a paper substrate

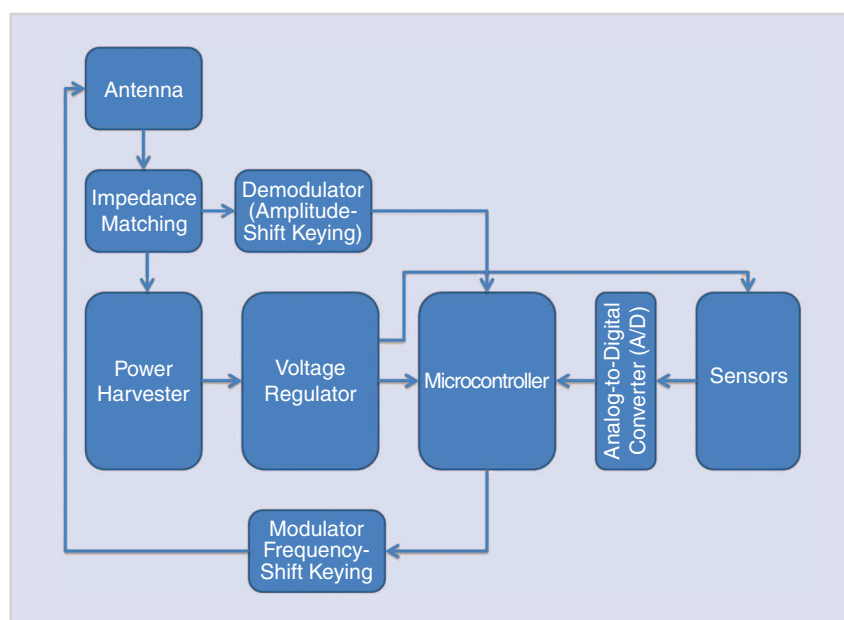
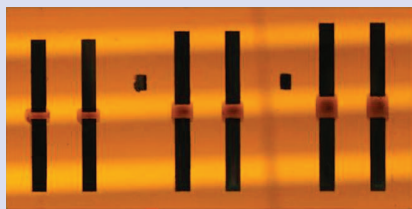
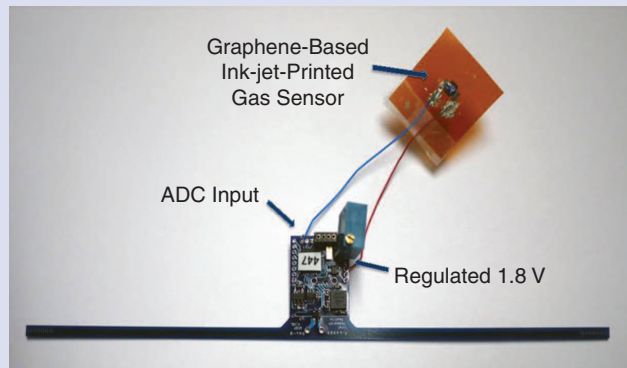


**FIGURE 7** A block diagram of the WISP RFID wireless sensor platform.



(a)



(b)

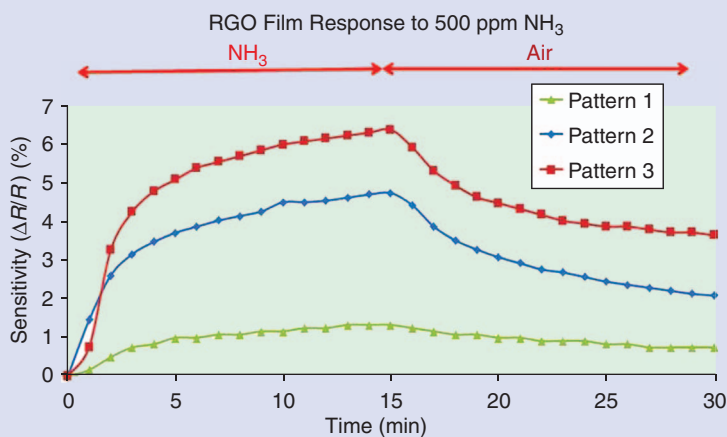
**FIGURE 8** (a) Three different dimension RGO patterns interfaced with silver nanoparticle conductive on Kapton and (b) an RGO-based WISP gas sensor.

- 2) curing and reduction of the GO thin film
- 3) alignment of the RGO film and printing of the antenna
- 4) sintering of the printed silver Cabot ink
- 5) integration of an RFID integrated circuit (IC) chip on the tag.

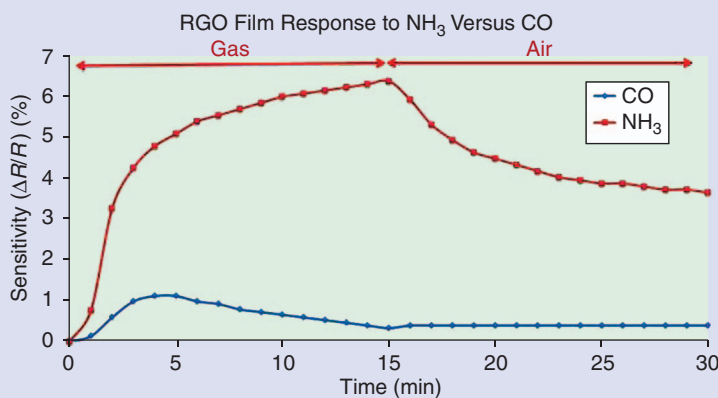
In step 2, after printing and curing, each sample was reduced to obtain the desired graphene from the GO. Scanning electron microscopy (SEM) was used to observe the overall quality of the graphene thin films (i.e., the presence of defects in the printed films, etc.) and to make adjustments in the processing of further prints. Figure 6 provides SEM images of both the initial GO and RGO thin films. The wrinkles on the surface of the samples shown in Figure 6 are typical characteristics of GO and RGO thin films, which are likely indicative of minor defects in the structure [18].

### RGO-BASED WIRELESS IDENTIFICATION AND SENSING PLATFORM GAS SENSOR

After the validation of the dc performance of ink-jet-printed RGO, we present the gas sensor prototype based on the RGO dc performance and the wireless identification and sensing platform (WISP), which is shown as an available off-the-shelf device that has been optimized for wireless sensing. The sensor prototype is a fully passive, battery-free, and programmable RFID tag that can be powered and read by off-the-shelf EPC Gen2 UHF RFID readers [2], [19]. It has an onboard microcontroller for sensing and computing functions and is a multifunctional platform. The block diagram of a WISP is shown in Figure 7, which includes power harvesting, sensors, signal processing, and modulation/demodulation capabilities. The WISP is



(a)



(b)

**FIGURE 9** (a) The measured response of RGO thin films in the presence of  $\text{NH}_3$  and (b) the measured response of RGO thin films to  $\text{NH}_3$  and CO.

solely powered by the RF energy illuminated by any commercial RFID reader. This RF energy from the reader is rectified by a charge pump topology consisting of diodes and capacitors to charge the onboard capacitor. Whenever located within the interrogation zone of an RFID reader, the WISP-gas sensor is automatically detected and begins the transmission of the sensed information through the EPC Gen2 protocol.

Recently reported RGO-based inks have enabled the implementation of an ink-jet-printed graphene gas detection sensor that has a very rapid recovery time and high sensitivity [2], [20]. As demonstrated in [2], GO, which is the precursor to graphene, is ink-jet printed onto an ultraviolet-ozone-treated Kapton substrate with silver contact pads. The printed GO is then inserted in postprocessing to reduce the GO to sheets of RGO. GO can be sintered using both heat and lasers [20].

The deposited graphene sensors are shown in Figure 8(a) with printed silver electrodes, which are used to connect the sensor with the WISP RFID tag. As the conductivity of the RGO changes upon exposure to gas, the graphene sensor is used in a resistor divider configuration with a fixed resistor, which is placed across the WISP's regulated 1.8-V and ground rails. When the WISP is interrogated by the reader, the voltage from the voltage divider circuit is read by the WISP's analog-to-digital converter (ADC), processed, and sent to the reader in the EPC Gen2 packet. The proposed WISP-based gas sensor was placed in an isolated gas chamber, as shown in Figure 8(b), to expose the sensor to  $\text{NH}_3$  and CO to measure the sensitivity. Figure 9(a) and (b) shows the extracted sensitivity, which is the change in the dc resistance of the sensor over the initial resistance. Resistance changes of up to 6% were realized with response times of fewer than 5 min when  $\text{NH}_3$  was applied. Upon the removal of the gas at  $t = 15$  min and the application of air, the sensors recover 30% of the change caused by the gas within 5 min. This allows for the reuse of the sensors, which is required for low-cost and long-term end solutions. Figure 9(b) shows the selectivity of the film between CO and

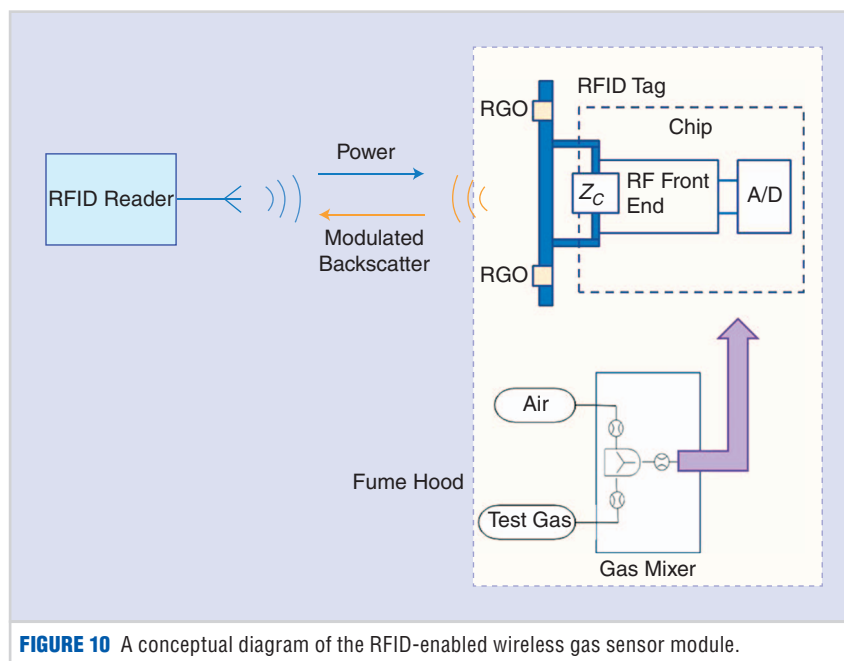


**FIGURE 10** A conceptual diagram of the RFID-enabled wireless gas sensor module.

$\text{NH}_3$ , showing a noticeable difference in the characteristic response of the sensor to each gas. This can be used in data analysis to back out the type of gas present and the exposure amount.

### RGO-BASED PASSIVE UHF RFID GAS SENSOR

The RFID reader sends an interrogating signal to the RFID tag, which consists of an antenna and an IC chip. The IC responds to the reader by varying the antenna input impedance, thereby modulating the backscattered radiation levels. The modulation scheme often used in RFID applications is amplitude shift

keying. The IC impedance switches between the matched and mismatched state, altering the levels of backscattered radiation [21]. As illustrated in Figure 10, the RGO thin film is integrated with the printed antenna by direct-write methods and acts as a tunable part of the antenna with an impedance value determined by the concentration of the target gas. The RFID reader monitors the backscattered power level. Once the power level changes, it shows that there is a variation of the RGO film impedance; therefore, the wireless sensor detects the existence and concentration of the target gas. The prototype of this type of sensor is shown in Figure 4.

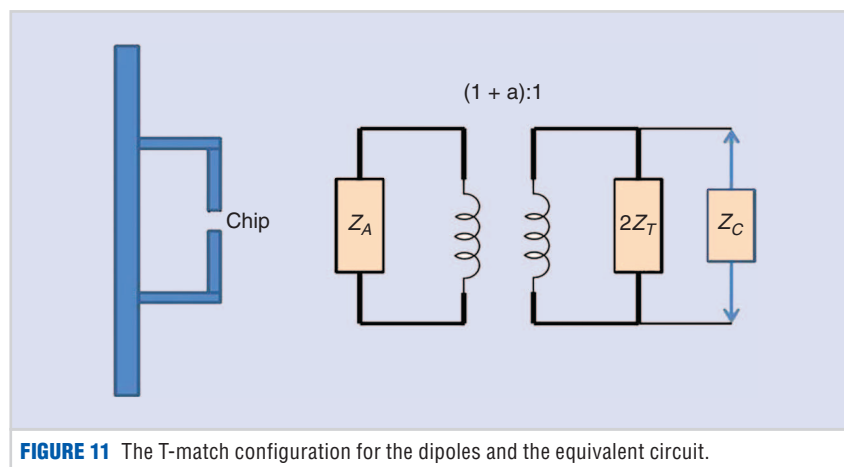


**FIGURE 11** The T-match configuration for the dipoles and the equivalent circuit.

The power level of the received signal can be calculated using the Friis free-space equation as

$$P_{\text{tag}} = P_t G_t G_r \left( \frac{\lambda}{4\pi d} \right)^2, \quad (1)$$

where  $P_t$  is the power transmitted from the reader antenna,  $G_t$  and  $G_r$  are the gains of the reader antenna and the antenna, respectively, and  $d$  is the distance between the reader and the tag.

The design goal for the tag antenna was to achieve an omnidirectional read pattern while maintaining a maximum read range. The maximum read range of a passive UHF RFID tag depends on the gain and quality of impedance matching between the tag antenna and IC [22]. The read range can be optimized by selecting an IC with low power consumption, maximizing the antenna gain, and arranging a complex conjugate impedance matching between the IC and tag antenna for maximal power transfer to the RFID IC [23]. The T-matching network is an effective way to modify the input impedance of a dipole by introducing a centered short-circuit stub, as shown in Figure 11 [24].

The tags were tested using a KIN-TEK FlexStream gas generator for the accurate gas concentrations. The measurement setup was capable of producing reliable mixtures of up to 50 ppm of nitrogen dioxide gas diluted in nitrogen gas. A Tagformance Lite RFID reader (Voyantic, Inc., 2011) is adopted for measuring the minimum required transmitted power to excite the RFID tag. At each frequency point, the reader varies the transmitting power from 30 dBm until the power is not able to activate the RFID chip. After the reader sweeps throughout the entire frequency range from 800 MHz to 1 GHz, the minimum required transmitted power level versus frequency curve can be obtained. When the impedance of the antenna-based sensor varies due to the gas exposure, the antenna resonant frequency changes accordingly. Therefore, gas sensing can be achieved using the relationship between the transmitted power to read the antenna-based sensor and gas concentration.

The tag presented in Figure 2 was exposed to 20 ppm  $\text{NH}_3$  for the gas test. After exposure to the target gas, the

mismatching of the impedance between the antenna and the IC chip caused the backscattered power level to be reduced as compared to the original power level around the 915 MHz target frequency. A 600% difference in the power level was observed at the target frequency by the received antenna in less than 1 min. This will be the foundation of the RFID-enabled, carbon-based smart skins for the gas sensing applications.

## SUMMARY AND OUTLOOK

Two sensing topologies have been presented for gas sensing for integration with smart skins. These sensors exhibit the important properties as zero-/low-power operation, high sensitivity, and even selectivity. Cognitive printed smart skins have the potential to greatly increase the safety and longevity of large structures and improve the quality of life in everyday environments such as grocery store food aisles and airport luggage safety checks. In addition, by using an industry standard RFID platform for sensing, we can leverage the low-cost, low-power benefits of the platform along with the ease of integration with current and future RFID installations.

## ABOUT THE AUTHORS

**Taoran Le** (taoran3@gatech.edu) is with the Georgia Institute of Technology, Atlanta.

**Ziyin Lin** (zylin@gatech.edu) is with the Georgia Institute of Technology, Atlanta.

**C.P. Wong** (cp.wong@mse.gatech.edu) is with the Georgia Institute of Technology, Atlanta.

**M.M. Tentzeris** (etentze@ece.gatech.edu) is with the Georgia Institute of Technology, Atlanta.

## REFERENCES

- [1] V. Lakafosis, X. Yi, T. Le, E. Gebara, Y. Wang, and M. M. Tentzeris, "Wireless sensing with smart skins," in *Proc. 2011 IEEE Sensors*, Oct. 2011, pp. 623–626.
- [2] T. Le, V. Lakafosis, Z. Lin, C. P. Wong, and M. M. Tentzeris, "Inkjet-printed graphene-based wireless gas sensor modules," in *Proc. IEEE 62nd Electronic Components and Technology Conf.*, 2012, pp. 1003–1008.
- [3] A. K. Geim and K. S. Novoselov, "The rise of graphene," *Nature Mater.*, vol. 6, no. 3, pp. 183–191, 2007.
- [4] A. Peigney, C. Laurent, E. Flahaut, R. R. Bacsa, and A. Rousset, "Specific surface area of carbon nanotubes and bundles of carbon nanotubes," *Carbon*, vol. 39, no. 4, pp. 507–514, 2001.

- [5] S. Stankovich, D. A. Dikin, R. D. Piner, K. A. Kohlhaas, A. Kleinhammes, Y. Jia, and R. S. Ruoff, "Synthesis of graphene-based nanosheets via chemical reduction of exfoliated graphite oxide," *Carbon*, vol. 45, no. 7, pp. 1558–1565, 2001.
- [6] F. Schedin, A. K. Geim, S. V. Morozov, E. W. Hill, P. Blake, M. I. Katsnelson, and K. S. Novoselov, "Detection of individual gas molecules adsorbed on graphene," *Nature Mater.*, vol. 6, no. 9, pp. 652–655, 2007.
- [7] D. Li, and R. B. Kaner, "Graphene-based materials," *Nat. Nanotechnol.*, vol. 3, p. 101, 2008.
- [8] Dimatix DMP 28XX PC Control Software, Fujifilm USA Dimatix Inc., Santa Clara, CA, 2008.
- [9] G. Wiederrecht, *Handbook of Nanofabrication*. New York: Elsevier, 2009.
- [10] L. Yang, A. Rida, R. Vyas, and M. M. Tentzeris, "RFID tag and RF structures on a paper substrate using inkjet-printing technology," *IEEE Trans. Microwave Theory Tech.*, vol. 55, no. 12, pp. 2894–2901, 2007.
- [11] B. S. Cook and A. Shamim, "Inkjet printing of novel wideband and high gain antennas on low-cost paper substrate," *IEEE Trans. Antennas Propag.*, vol. 60, no. 9, pp. 4148–4156, 2012.
- [12] M. L. Allen, M. Aronniemi, T. Mattila, A. Alastalo, K. Ojanpera, M. Suhonen, and H. Seppa, "Electrical sintering of nanoparticle structures," *Nanotechnology*, vol. 19, no. 17, pp. 1–4, 2008.
- [13] P. Laakso, S. Ruotsalainen, E. Halonen, M. Mntysalo, and A. Kempainen, "Sintering of printed nanoparticle structures using laser treatment," VTT Tech. Res. Centre Finland, Espoo, Finland, Tech. Rep., 2009.
- [14] L. Yang, A. Rida, and M. M. Tentzeris, "Design and development of radio frequency identification and RFID-enabled sensors on flexible low cost substrates," *Synth. Lect. RF/Microwaves*, vol. 1, no. 1, pp. 1–89, 2009.
- [15] J. Vaillancourt, "All ink-jet-printed carbon nanotube thin-film transistor on a polyimide substrate with an ultrahigh operating frequency of over 5 GHz," *Appl. Phys. Lett.*, vol. 93, no. 24, p. 243301, 2008.
- [16] R. Vyas, V. Lakafosis, H. Lee, G. Shaker, L. Yang, G. Orecchini, A. Traille, M. Tentzeris, and L. Roselli, "Inkjet printed, self powered, wireless sensors for environmental, gas, and authentication-based sensing," *IEEE Sensors. J.*, vol. 11, no. 12, pp. 3139–3152, 2011.
- [17] Z. Lin, Y. Yao, Z. Li, Y. Liu, Z. Li, and C. P. Wong, "Solvent-assisted thermal reduction of graphite oxide," *J. Phys. Chem. C*, vol. 114, no. 35, pp. 14819–14825, 2010.
- [18] O. C. Compton and S. T. Nguyen, "Graphene oxide, highly reduced graphene oxide, and graphene: Versatile building blocks for carbon based materials," *Small*, vol. 6, no. 6, pp. 711–723, 2010.
- [19] L. Yang, R. Zhang, D. Staiulescu, C. P. Wong, and M. M. Tentzeris, "A novel conformal RFID-enabled module utilizing inkjet-printed antennas and carbon nanotubes for gas-detection applications," *IEEE Antennas Wireless Propag. Lett.*, vol. 8, pp. 653–656, 2009.
- [20] L. Le, "Graphene supercapacitor electrodes fabricated by inkjet printing and thermal reduction of graphene oxide," *Electrochem. Commun.*, vol. 13, no. 4, pp. 355–358, 2011.
- [21] P. V. Nikitin and K. V. S. Rao, "Performance limitations of passive UHF RFID systems," in *Proc. IEEE Antennas and Propagation Society Int. Symp.*, vol. 1011, July 2006.
- [22] K. S. Rao, P. V. Nikitin, and S. F. Lam, "Antenna design for UHF RFID tags: A review and a practical application," *IEEE Trans. Antennas Propag.*, vol. 53, no. 12, pp. 3870–3876, 2005.
- [23] K. Kurokawa, "Power waves and the scattering matrix," *IEEE Trans. Microwave Theory Tech.*, vol. 13, no. 2, pp. 194–202, 1965.
- [24] C. A. Balanis, *Antenna Theory: Analysis and Design*. Hoboken, NJ: Wiley, 2012.